Effect of Gas Pressure on the Collisional Line Width and Line Shift in Graphite Furnace Atomic Absorption Spectrometry

Jing-Chyi Chang and Thomas C. O'Haver
Department of Chemistry and Biochemistry, University of Maryland, College Park, MD 20742, USA

The collisional line width of the resonance atomic absorption lines of Ca, Cu and In have been measured in graphite furnace atomisers by means of a wavelength modulated échelle spectrometer and a measurement method based on transmission profile fitting. A measurement precision of ±0.1 pm is observed for Cu (324.754 nm) based on growth curve shapes measured in peak area or peak height. Time resolved line widths within a single atomisation have been measured for Ca (422.673 nm) and for In (410.176 nm), with a time resolution of 0.3 s and a precision of ±0.5 pm. This measurement precision is sufficient to show clearly the effect of increased gas pressure on the line width and the line shift. Collisional cross-sections for In and Ca are estimated from the effect of pressure on the line widths and shifts and are compared with previously published values obtained using theoretical calculations.

Keywords: *Atomic absorption spectrometry; continuum; line width; pressure; collision*

The importance of fundamental reference data in atomic spectroscopy has been pointed out recently by Lovett[1] and by Scheeline.[2] Atomic line profiles are among the important fundamental reference data for theoretical study in atomic spectroscopy, such as for the calculation of the absolute number density of the analyte or simulation of the behaviour of atomic absorption in graphite furnace atomic absorption spectrometry.[3,4] Moreover, the relative position and width of the emission line of the light source [usually a hollow-cathode lamp (HCL)] and the absorption line of the analyte atoms in the atomiser influence the sensitivity and the linearity of the analytical curve in line source atomic absorption (AA). So far, the most common techniques employed for line-profile measurements have been either indirect methods such as the curve of growth method[5–11] or direct methods based on Zeeman scanning,[12–17] Fabry - Perot interferometry scanning,[18–36] échelle spectrometer scanning[37–47] and Fourier transform spectrometry.[48] Most of these measurements are devoted to emission profiles such as electrodeless discharge lamps, HCLs, flame or inductively coupled plasmas; few measurements of absorption profiles in analytical atomisers have been reported. In addition, very few measurements of absorbance line profiles have been carried out in a graphite furnace because of the difficulties of measuring a rapid transient spectral profile. Emission profiles have been measured inside the graphite furnace by using a wavelength modulation échelle spectrometer,[45] but no correction was made for the spectrometer slit function.

The effect of the gas pressure in the atom cell has been studied by several workers[49–56] using line-source instrumentation, but no direct measurement of the absorption line profile width and line shift related to pressure has been reported in analytical atomisers. Fazakas and co-workers[50–54] have studied the effect of atomisation pressure on the measuring sensitivity and on line-overlap interferences in line-source AAS and have interpreted the effects in terms of collisional line broadening and shift. However, no direct measurements of line width or shift were reported. Increasing the gas pressure is expected to have both spectroscopic effects (a shift in the wavelength of the line centre, an increase in the collisional contribution to the absorption line width and a reduction in the calibration graph non-linearity) and physiochemical effects (a reduction in the diffusion rate of atoms and a delay in the absorption - time pulse). On the other hand, reducing the pressure should have the opposite effect. Operation at pressures below atmospheric pressure has been observed to increase the curvature of the calibration graph, sharpen the absorbance - time pulse and reduce the memory effects, matrix effects and peak tailing of refractory analytes.[56]

In this work a method for measuring absorption line widths in graphite furnace atomisers is described and used to observe the effect of gas pressure on the collisional width and shift of the resonance absorption line of Ca and In.

Theory

In a continuum-source AA measurement, the spectral profile of the transmitted light $I(\lambda)$ may be written

$$I(\lambda) = I_o(\lambda)[S(\lambda)*10^{-A_i a(\lambda)} + \alpha_s] \quad \ldots \quad \ldots \quad (1)$$

where $I_o(\lambda)$ is the spectral profile of the incident light, $S(\lambda)$ is the spectrometer slit function, the symbol * denotes convolution, A_i is the intrinsic absorbance (that is, the "true" absorbance at the line centre that would, in principle, be measured by an instrument that has infinite resolution, zero stray light and infinite dynamic range), $a(\lambda)$ is the absorption profile normalised to a peak height of unity and α_s is the fractional unabsorbed stray light. This equation predicts the transmission profile that would be measured experimentally by scanning the spectral distribution of the light source across the absorption line. In the present work this measurement is done by means of a tunable high-resolution monochromator and a continuum primary source, but in principle it could be done by a tunable line source, such as a tunable laser or Zeeman-tuned HCL. (However, a conventional line-source AA system cannot be used to acquire this type of data.)

The assumption is made here that the absorption profile $a(\lambda)$ can be approximated by the convolution of a Gaussian Doppler contribution, which is calculated from the atomiser temperature and the relative atomic mass of the analyte, and a Lorentzian collisional contribution, whose width is to be determined. If $S(\lambda)$, $a(\lambda)$ and α_s in equation (1) are determined beforehand, the intrinsic absorbance A_i can be measured indirectly by adjusting it until the calculated $I(\lambda)$ is a best fit to the experimentally observed transmission profile. Absorbances measured in this way in analytical flames have been found to be linear over very wide concentration ranges, even in the optically thick region.[11] The collisional line width can also be determined in the following way. A model for the absorption profile $a(\lambda)$ is constructed, based on a Gaussian Doppler contribution (which can be calculated with sufficient accuracy from the atomiser temperature and the relative atomic mass of the analyte) and a Lorentzian collisional contribution with an adjustable collisional line width. The

collisional line width and intrinsic absorbance A_i are adjusted until the calculated $I(\lambda)$ is a best fit to the experimentally observed transmission profile. This is referred to as the direct curve fitting method. This method can also be used to measure wavelength shifts, by allowing the peak centre wavelength to be a variable in the fitting procedure.

A more accurate procedure for line-width measurement, reported in detail previously,[11] requires the measurement of the transmission profiles from a set of standard solutions of known concentration. From this set of profiles, a series of intrinsic absorbance analytical curves are constructed for various trial values of the line width, and the line width that gives the most linear curve is taken as the measured value. This is referred to as the analytical-curve method. This procedure works effectively only if the significant sources of analytical curve non-linearity are optical effects (*i.e.*, finite spectral bandpass and stray light) and if the chemical sources of curvature are negligible. The analytical-curve method requires at least two profiles at different known concentrations, whereas the direct curve fitting method requires only a single transmission profile [in practice, the ensemble average of several successive profiles is usually used to improve the signal to noise (S/N) ratio]. For determining the time-resolved variations in line width during a single atomisation, only the direct method is practical.

The known hyperfine components of Cu and In were used to synthesise their total absorption profiles, based on the relative peak absorbances and spacings of the 12 components of Cu 324.754 nm and 8 components of In 410.176 nm, as reported by de Galan and co-workers.[28,29]

Lovett and Parsons[57] have developed a simple theory that allows the theoretical calculation of optical cross-sections and collisional widths and shifts for transitions of interest in atomic absorption. The collisional width $\Delta\nu_c$ is given by

$$\Delta\nu_c = n\sigma v \quad . . \quad . . \quad . . \quad (2)$$

where n is the number density of perturbers (*i.e.*, colliding gas molecules), σ is the collision cross-section and v is the mean velocity of the absorber - perturber pair (which depends only on the temperature and the masses of the analyte and perturber). The number density n can be calculated from the ideal gas law, which yields:

$$\Delta\nu_c = \frac{N_o\sigma v}{RT}P \quad . . \quad . . \quad . . \quad (3)$$

where N_o is Avogadro's number. The collisional width $\Delta\nu_c$ should therefore be proportional to pressure and it should be possible to determine the collisional cross-section σ from the slope of experimental $\Delta\nu_c$ *versus* P plots. The slope is also expected to be a function of temperature; if the cross-section σ is constant, the slope would be inversely proportional to the square root of the absolute temperature.

Experimental

The spectrometer system has been described previously[58] and is used in the present work without change. For this work the modulation frequency was 48 Hz and the slit width and height were 25 and 500 μm, respectively.

Two types of electrothermal atomisers were utilised. A Perkin Elmer HGA-500 graphite furnace equipped with an AS-1 autosampler was used to perform the calibration curve measurements. The pressurised atomisation experiments were performed with an Instrumentation Laboratory 555 CTF atomiser in the temperature feedback mode. The gas pressure was read from the pressure gauge in the 555 CTF atomiser controller. A 20-μl aliquot of analyte was dispensed into the graphite tube throughout this work. High-purity argon was used as the purge gas. The Perkin Elmer atomiser was operated in the gas-stop mode during atomisation. A flow-rate of 1 l min^{-1} was maintained during the atomisation stage for all pressures in the IL 555 CTF atomiser. For both atomisers, the ashing temperature is 550 °C for Ca, 600 °C for In and 500 °C for Cu, and the atomisation temperature is 2100 °C for both Ca and In, and 2700 °C for Cu. The ramp time from ashing to atomisation was set to zero for all elements. The graphite tube temperature was monitored with an Ircon Series 1100 automatic optical pyrometer. The heating of the fill gas during atomisation in the IL 555 CTF atomiser was not observed to change the gas pressure significantly, presumably due to the buffering effect of the relatively large volume of unheated gas in the remainder of the atomiser enclosure and in the connecting tubing.

Fig. 1 shows a typical three-dimensional (intensity - wavelength - time) surface plot for several different concentrations (20 μl volumes) of Cu atomised at atmospheric pressure. The wavelength axis extends over a 42 pm interval centred on the 324.754-nm resonance line. Each point in the wavelength direction corresponds to 1.5 pm. Each slice in the time direction is the average of ten successive modulation cycles and represents 0.2 s of atomisation time. Altogether, 20 time-slice profiles were plotted for each atomisation. The time lapse between atomisations is not shown to scale.

The spectrometer slit function and the unabsorbed stray light fraction are instrumental constants that depend on the spectrometer settings (wavelength, slit-width and slit-height)

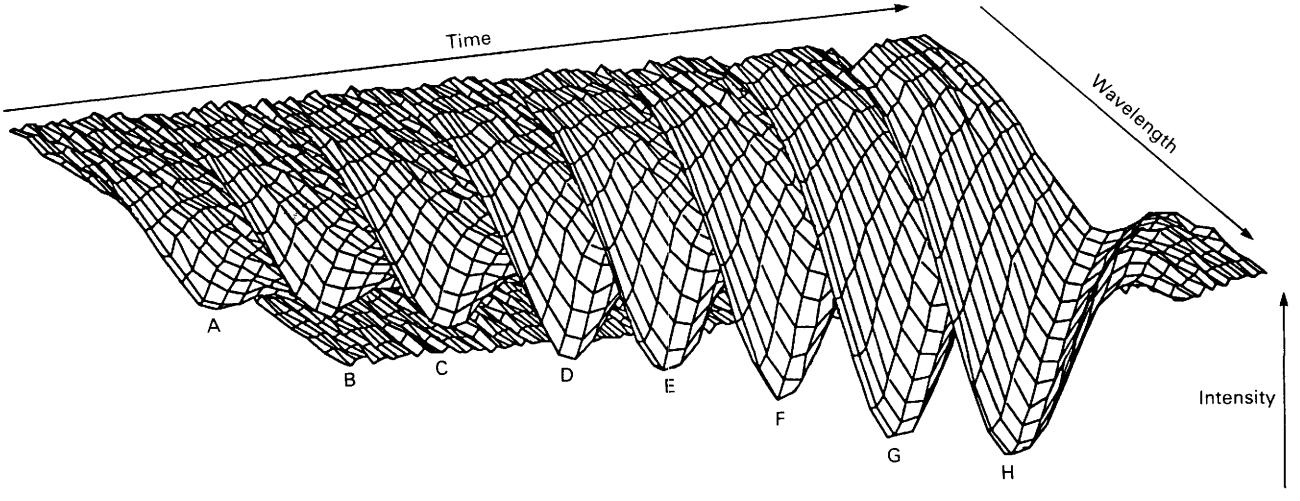

Fig. 1. Intensity - wavelength - time surface plot for eight different concentrations for Cu atomised at atmospheric pressure in a Perkin Elmer HGA-500 graphite furnace atomiser. Cu concentrations: A, 16; B, 24; C, 32; D, 63; E, 91; F, 167; G, 500; and H, 1000 p.p.b. The wavelength axis extends over a 42 pm interval centred on the 324.754-nm resonance line. Each slice in the time direction is the average of ten successive modulation cycles and represents 0.2 s of atomisation time

and are assumed to be independent of analyte concentration.[11] The spectrometer slit function was determined by scanning emission profiles of a Ca HCL operated at different currents and then fitting them with a Gaussian function. The resulting Gaussian widths were extrapolated to zero lamp current to avoid the effect of self-absorption. This procedure gave a spectral bandpass at 422 nm of 9.5 pm with a 25-μm slit-width and 11.8 pm with a 50-μm slit. The spectral bandpass of the échelle spectrometer is inversely proportional to the diffraction order in which the desired wavelength falls. The spectral bandpasses for Cu (8.7 pm at a 50-μm slit-width) and In (9.1 pm at a 25-μm slit-width) were calculated accordingly.

The unabsorbed stray light fraction α_s for each element studied was determined by atomising a very high concentration of analyte solution and measuring the ratio of the minimum intensity transmitted at the line centre to the incident intensity at that wavelength. The fractional stray light was found to be 0.053 (*i.e.*, 5.3%) at 324 nm, 0.053 at 422 nm and 0.054 at 410 nm.

Results and Discussion

The four parameters in equation (1) that remain to be determined by curve fitting are collisional line width, line centre wavelength, intrinsic absorbance and background intensity I_0. (The background intensity can in principle be measured separately, but in practice it is treated as an adjustable parameter to compensate for source intensity drift.) A general problem that occurs in curve-fitting peak-type signals when width and height are both variable parameters is the inverse correlation between width and height; *i.e.*, an under-estimation of width is compensated for by an over-estimation of height. This problem is made worse in the present application by the comparatively large spectrometer spectral bandpass relative to the line width to be measured. (If the spectral bandpass was much larger than the line width, then the measured signal would have a shape determined only by the spectrometer slit function and its amplitude would be determined by the peak area, *i.e.*, the product of width and height; it would then be impossible to extract unique values of width or height individually.) Fig. 2 shows a contour plot of a typical fitting error surface encountered in this work. This is for a computer-synthesised transmission profile model with a collisional (Lorentzian) line width of 2 pm, a Gaussian spectral bandpass of 10 pm, an intrinsic absorbance of 0.6 and a photon noise level similar to that of typical experimental data. The inverse correlation between intrinsic absorbance and line width results in a shallow valley with several local minima in the response surface. The X symbols are the results of a Monte Carlo simulation of 50 repeated fits of the same model with different sets of simulated photon noise. (In that simulation, the line centre wavelength and background intensity were also treated as adjustable values in the curve-fitting procedure, but the best-fit values of those parameters are not reported here because they behave as expected and are not strongly correlated with the other parameters.) Note that the distribution of best-fit values tend to fall along the "floor" of this valley. Based on simulations of this type and on the observation of a large number of experimental measurements, the precision of line-width measurement by direct curve fitting has been found to be ±0.5 pm.

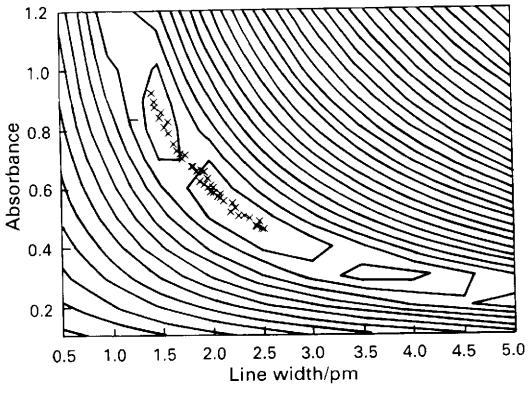

Fig. 2. Contour plot of the fitting error surface of a synthesised transmission model with a collisional line width of 2 pm, an intrinsic absorbance of 0.6, a spectral bandpass of 10 and a noise level similar to that of the experimental data. This illustrates the strong inverse correlation between intrinsic absorbance and line width that results in a very shallow valley with several local minima in the response surface. The X symbols are the results of a Monte Carlo simulation of 50 repeated fits with different sets of simulated photon noise

Assuming that the absorption line width is independent of concentration and therefore absorbance (*i.e.*, no resonance broadening), it should be possible to choose any arbitrary concentration for the width measurement. In fact, it is a useful test of internal consistency to check for the agreement of widths measured at two different concentrations. The optimum concentration range is limited on the low end by the S/N and on the high end by the increase in the correlation between the line width and the absorbance, which has been called "concentration broadening".[59] A similar correlation can exist

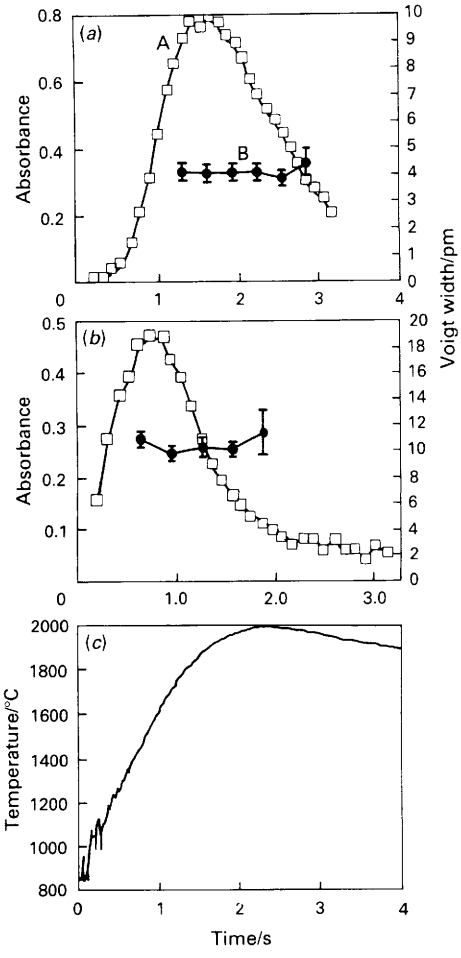

Fig. 3. Time resolved line widths (curve A) *versus* time, measured by direct curve fitting, for the graphite furnace atomisation of (*a*) 0.8 ng of Ca (422.673 nm) and (*b*) 6.8 ng of In (410.176 nm), superimposed on the absorbance - time signal (curve B). Each line width is the average of ten repeated atomisations; the standard deviations are shown by the error bars. The precision of the width measurement is seriously degraded if the absorbance is less than about 0.2. The measurement precision degrades if the absorbance falls below about 0.2, but there seems to be no significant systematic variation of line width with time over this time period. (*c*) Atomiser temperature as a function of time, measured by means of an optical pyrometer

at high concentrations between the absorbance and the background intensity I_0, particularly if the modulation interval is not large enough. These problems can be minimised by adjusting the solution concentration so that the intrinsic absorbance falls below about 1, but not so low as to degrade the S/N. The optimum absorbance seems to be in the range 0.3–1.

The measurement of time-resolved line widths required that the transmission profiles be measured and fit at a sequence of times (and therefore different atom concentrations) during one atomisation. As a compromise between time resolution and S/N, the measured transmission profiles are divided into 0.3-s groups and averaged. Fig. 3(*a*) shows the line width *versus* time, measured by direct curve fitting, for the graphite furnace atomisation of 0.8 ng of Ca (422.673 nm), superimposed on the absorbance - time signal. Each point is the average of the line widths measured from ten repeated atomisations; the standard deviations are shown by the error bars. There appears to be no significant systematic variation of line width with time over this time period. The atomiser temperature, measured by optical pyrometry, is shown in Fig. 3(*b*). Over the time period within which the Ca line width is measured, the atomiser temperature varies from 1590 to 1975 °C, the theoretical Doppler width increases by 0.2 pm, from 2.2 to 2.4 pm, and the theoretical collisional width at 1 atm, based on the Lovett and Parsons equations[57] and using a cross-section of 7×10^{-15} cm^2, decreases from 2.1 to 1.9 pm. Considering that the precision of the total line width measurements is about ±0.5 pm, it is not surprising that the effect of this temperature variation on the total line width is too small to observe in these data. Measurements of In (410.176 nm) show similar behaviour [Fig. 3(*c*)], but in this instance the temperature variation is larger (1350–1880 °C) because In is more volatile. Over this temperature range the calculated Doppler width increases by 0.2 pm, from 1.1 to 1.3 pm and the theoretical collisional width at 1 atm, using a cross-section of 1×10^{-14} cm^2, decreases from 3.3 to 3.1 pm. Despite the larger temperature variation, the expected variation in the Doppler and collisional widths due to temperature is still smaller than the experimental measurement precision.

Attempts to measure the line widths at times earlier than 1.3 s for Ca and 0.6 s for In were unsuccessful due to the rapid change of absorbance with time during the leading edge of the absorption - time pulse.

A potential source of systematic error in the direct curve-fitting procedure is caused by the correlation between the line width and the spectral bandpass of the spectrometer. As described above, the spectrometer bandpass is measured separately and is not included as one of the adjustable parameters in the curve-fitting procedure. Ideally, if the spectrometer bandpass is measured accurately, it will not bias the final results. However, a given error in the estimation of the spectrometer bandpass will bias the line-width measurement by the same absolute amount. The accuracy of the spectrometer bandpass measurement is estimated to be about ±1 pm. This difficulty could be reduced by using a spectrometer with a much higher resolution. The échelle spectrometer used in this work has a spectral bandpass that is typically about two to three times the total absorption line width. When combined with the fitting uncertainty due to random noise, the over-all uncertainty of time-resolved line widths measured by the direct curve fitting method is estimated to be about ±2 pm.

An alternative method of line-width measurement, the analytical curve method, has been shown to be much less sensitive to bias resulting from errors in the measurement of the spectral bandpass.[11] This method has been successfuly applied to measurement of the absorption line width of Cu 324.754 nm in a graphite furnace. Log - log plots of the experimental analytical calibration curve (intrinsic absorbance *versus* mass of Cu) are shown in Fig. 4(*a*) for peak area and in 4(*b*) for peak height. The slope of the log - log analytical curve near an intrinsic absorbance of 1.0 is measured as a function of the value of the line width that is used to determine the intrinsic absorbance, and the line width at which the slope is unity is taken as the measured value. This procedure gives a value of 2.2 ± 0.1 pm for either peak-height or peak-area measurement, where the uncertainity is determined by repeating the procedure with different sub-sets of the calibration set. The same method applied to the measurement of the Voigt width of Cu in an air - acetylene flame gave a value of 2.1 ± 0.1 pm, which is not significantly different from the furnace value, as expected. On the basis of the equations of Lovett and Parson[57] the difference between the collision cross-sections with Ar and with N_2 is expected to be less than 5% relative, not sufficient to be seen in the measurements made in the present study. The calibration curve method works satisfactorily in the air - acetylene flame for all the elements tested so far,[11] but it does not always work effectively in furnace atomisation. For example, the Ca calibration curve is significantly concave at high concentrations due to chemical effects. Therefore, this element does not exhibit the characteristic sigmoidal curve shapes (Fig. 4) that are observed when the trial collisional width is varied.

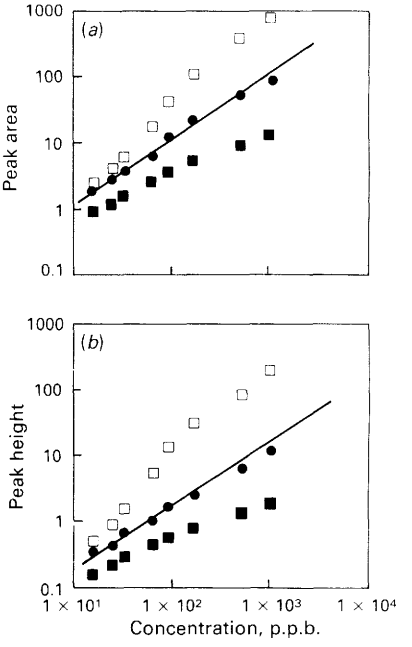

Fig. 4. Log - log plots of experimental analytical calibration curve of Cu, 324.754 nm (intrinsic absorbance *versus* mass of Cu) is shown: (*a*) for peak area; and (*b*) for peak height. Voigt widths: □, 1.7; ●, 2.1; and ■, 4.3 pm

Line-shift measurements are actually easier to make than line-width measurements, because there is little correlation between the line position and the other parameters in the curve-fitting model and because the fairly large spectral bandpass of the spectrometer does not affect the line position of the raw signal. The only problem is the wavelength drift of the échelle spectrometer, which can be 2–3 pm over a period of 4–5 hours. This problem is avoided by careful designing of the experiment; the spectrometer is allowed to warm up completely and the drift is checked before and after each series of measurements by measuring the profile of an HCL.

Effect of Gas Pressure

Transmission profiles of 6.8 ng of In (410.176 nm) and 0.8 ng of Ca (422.673 nm) were measured at four different Ar gas pressures in the IL 555 CTF atomiser. Profiles were measured at 0.3 s time intervals over the period 1.25–2.5 s for Ca and

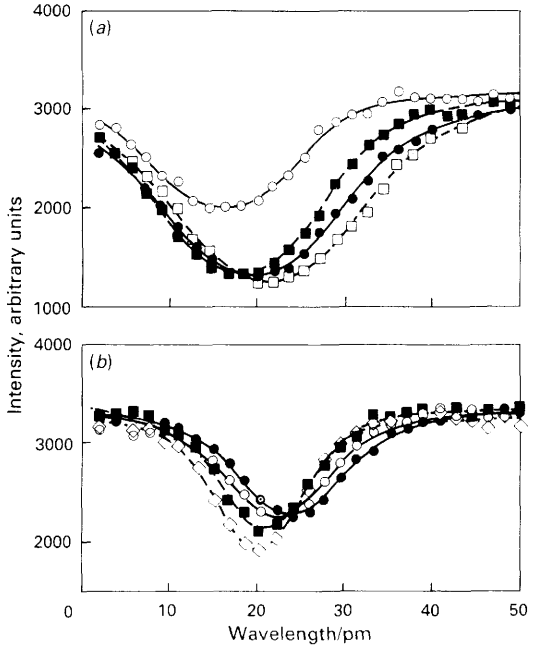

Fig. 5. Transmission profiles of (*a*) 6.8 ng of In (410.176 nm, monochromator spectral bandpass 9.1 pm) and (*b*) 0.8 ng of Ca (422.673 nm, monochromator spectral bandpass 9.5 pm) measured at four different pressures in the IL 555 CTF atomiser: (*a*) □, 3.5; ●, 2.9; ■, 1.9; ○, 1.0 atm; and (*b*) ●, 4.4; ○, 3.6; ■, 2.5; and □, 1.7 atm. Each of these profiles is averaged over a 0.3 s time interval near the absorption maximum. The increase in line width and the shift of the peak wavelength to longer wavelengths are caused by the increased collisional broadening with increasing pressure

0.6–1.6 s for In. Fig. 5 shows the profiles measured at the peak of each absorbance - time pulse. (The time to maximum absorbance was found to be independent of pressure for Ca and to increase slightly with pressure for In.) The increase in line broadening and the shift of the peak wavelength to longer wavelengths with increasing pressure are clearly observed even in these raw transmission profiles, despite the fact that they are substantially broader than the actual absorption line widths because of instrumental broadening. Most of the apparent width of the In absorption is actually due to unresolved hyperfine structure.

Each of the measured transmission profiles was submitted to the direct curve fitting procedure to determine the collisional width. Plots of width *versus* pressure were constructed for each time interval during the atomisation, and the collisional cross-sections were determined from equation (3). The collisional widths and cross-sections determined at the different time intervals were not found to be significantly different and were therefore pooled. Fig. 6 shows the pooled collisional widths as a function of gas pressure for both In (A) and Ca (B). The points and error bars represent the average and standard deviation of the pooled data. The solid lines are linear least squares fits. In both instances reasonably good fits to the expected linear relationship are obtained, but the intercept at zero pressure for the In data is far from zero. Part of this can be assigned to statistical uncertainty (the confidence interval of the intercept is ±1 pm), but a more important uncertainty is the spectral bandpass, which was calculated by extrapolation from the measured value for Ca rather than being measured directly. An error in the spectral bandpass is expected to bias the measured line width by an amount equal to the error. However, because the spectral bandpass is independent of pressure, any fixed error in this parameter should have no effect on the slope. (It is also possible that the assumption that the hyperfine spacings and amplitudes are independent of pressure may not be correct, but this is impossible to determine with the present apparatus

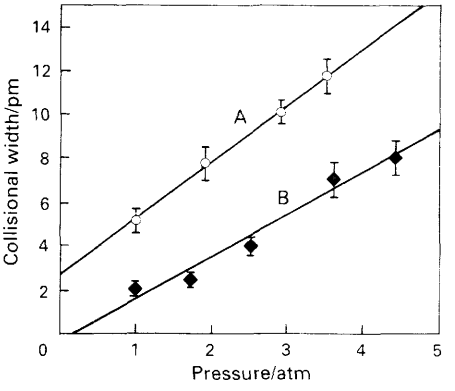

Fig. 6. Collisional width as a function of gas pressure for A, In and B, Ca, measured by the direct curve fitting method, assuming that the Doppler width is independent of pressure

Table 1. Comparison of experimental and theoretical collisional cross-sections, in cm^2, for In and Ca

Method of calculation	In	Ca
From slope of width *versus* pressure	$1.0 \pm 0.1 \times 10^{-14}$	$5.5 \pm 0.5 \times 10^{-15}$
From slope of shift *versus* pressure	1.2×10^{-14}	5.7×10^{-15}
From theory (reference 57)	1.07×10^{-14}	6.8×10^{-15}

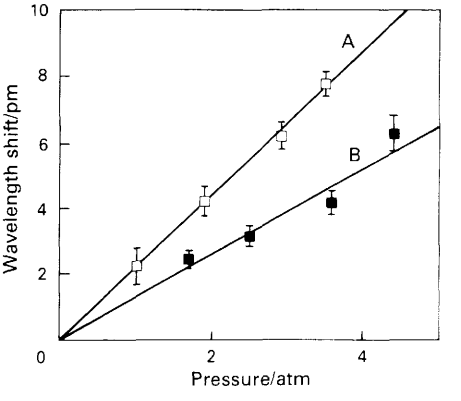

Fig. 7. Wavelength shift of the absorption line in pm, relative to the wavelength of the HCL line, for A, In and B, Ca

due to insufficient resolution.) The collisional cross-sections calculated from the slopes of these lines, according to equation (3), are summarised in Table 1. The confidence interval on these cross-sections expresses the range of cross-sections calculated from the widths measured at various times across the atomisation profile.

Fig. 7 shows the wavelength shift of the absorption line in pm, relative to the wavelength of the HCL line. The error bars represent the standard deviation of ten repeat atomisations at each pressure. The solid lines are linear least squares fits. The collisional cross-sections determined from the slopes of the least-squares lines are summarised in Table 1. The cross-section determined from the shift *versus* pressure data is in good agreement with that from the width *versus* pressure data. Both are compared in Table 1 with the theoretical calculations of Lovett and Parsons[57] for air - acetylene flames, adjusted according to their equations for the difference in temperature and perturber polarisibility and mass.

The transmission profiles in Fig. 5 show that the gas pressure also affects the magnitude of the absorption. Indium exhibits a substantial increase in absorption at increased pressure, whereas Ca exhibits a slight decrease. The effect of pressure is determined by the balance of two opposing factors. At increased pressure the collisional width is increased and

therefore the peak absorption is reduced. On the other hand, the gas diffusion rate is reduced at increased pressure. If the loss of absorbing atoms during the atomisation period occurs mainly by diffusion, then increasing the gas pressure should increase the atom residence time and thereby increase the area under the absorbance - time signal. For In, the decrease in peak absorption caused by line broadening is clearly outweighed by the increase in residence time. For Ca, the atom loss mechanisms seem to be little effected by pressure, because the area under the spectral absorption profile is approximately constant with increasing pressure, as would be expected for a fixed number of absorbing atoms.

The authors thank J. Harnly and N. Miller-Ihli for the use of their laboratory facilities for a portion of these studies.

References

1. Lovett, R. J., *Spectrochim. Acta, Part B*, 1988, **43**, 25.
2. Scheeline, A., *Spectrochim. Acta, Part B*, 1988, **43**, 57.
3. L'vov, B. V., Nikolaev, V. G., Norman, E. A., Polzik, L. K., and Mojica, M., *Spectrochim. Acta, Part B*, 1986, **41**, 1043.
4. Rutledge, M. J., Smith, B. W., and Winefordner, J. D., *Anal. Chem.*, 1987, **59**, 1794.
5. Hinnov, E., and Kohn, H., *J. Opt. Soc. Am.*, 1957, **47**, 151 and 156.
6. Hofmann, F. W., and Kohn, H., *J. Opt. Soc. Am.*, 1961, **51**, 512.
7. van Trigt, C., Hollander, Tj., and Alkemade, C. Th. J., *J. Quant. Spectrosc. Radiat. Transfer*, 1965, **5**, 813.
8. McGee, W. W., and Winefordner, J. D., *J. Quant. Spectrosc. Radiat. Transfer*, 1967, **7**, 261.
9. Townsend, W. P., Smyly, D. S., Zeegers, P. J., Svoboda, V., and Winefordner, J. D., *Spectrochim. Acta, Part B*, 1971, **26**, 595.
10. Browner, R. F., and Winefordner, J. D., *Anal. Chem.*, 1972, **44**, 247.
11. O'Haver, T. C., and Chang, J.-C., *Spectrochim. Acta, Part B*, 1989, **44**, 795.
12. Hollander, Tj., and Broida, H. P., *J. Quant. Spectrosc. Radiat. Transfer*, 1967, **7**, 965.
13. Hollander, Tj., and Broida, H. P., *Combust. Flame*, 1969, **13**, 63.
14. van Heek, H. F., *Spectrochim. Acta, Part B*, 1970, **25**, 107.
15. Hollander, Tj., Jansen, B. J., Plaat, J. J., and Alkemade, C. Th. J., *J. Quant. Spectrosc. Radiat. Transfer*, 1970, **10**, 1301.
16. Jansen, B. J., Hollander, Tj., and Alkemade, C. Th. J., *J. Quant. Spectrosc. Radiat. Transfer*, 1977, **17**, 695.
17. Koizumi, H., Oishi, K., and Yasuda, K., *Appl. Phys. Lett.*, 1982, **40**, 122.
18. Behmenburg, W., *J. Quant. Spectrosc. Radiat. Transfer*, 1964, **4**, 177.
19. Yasuda, K., *Anal. Chem.*, 1966, **38**, 592.
20. Davies, D. K., *J. Appl. Phys.*, 1967, **38**, 4713.
21. Kleinmann, I., and Cajko, J., *Spectrochim. Acta*, 1970, **25**, 657.
22. Kreege, W. C., and Roesler, F. L., *J. Opt. Soc. Am.*, 1970, **60**, 1100.
23. Human, H. G. C., and Butler, L. R. P., *Spectrochim. Acta, Part B*, 1970, **25**, 647.
24. Kirkbright, G. F., and Sargent, M., *Spectrochim. Acta, Part B*, 1970, **25**, 577.
25. Bruce, C. F., and Hannaford, P., *Spectrochim. Acta, Part B*, 1971, **26**, 207.
26. Kirkbright, G. F., Troccoli, O. E., and Vetter, S., *Spectrochim. Acta, Part B*, 1973, **28**, 1.
27. Kirkbright, G. F., and Troccoli, O. E., *Spectrochim. Acta, Part B*, 1973, **28**, 33.
28. Wagenaar, H. C., and de Galan, L., *Spectrochim. Acta, Part B*, 1973, **28**, 157.
29. Wagenaar, H. C., Pickford, C. J., and de Galan, L., *Spectrochim. Acta, Part B*, 1974, **29**, 211.
30. Human, H. G. C., and Scott, R. H., *Spectrochim. Acta, Part B*, 1976, **31**, 459.
31. Jansen, B. J., Hollander, Tj., and Alkemade, C. Th. J., *J. Quant. Spectrosc. Radiat. Transfer*, 1977, **17**, 695.
32. Walters, P. E., and Smit, K. J., *Spectrochim. Acta, Part B*, 1981, **36**, 333.
33. Mohamad, S. Z., and Petrakiev, A., *Spectrosc. Lett.*, 1981, **14**, 47.
34. Falk, H., *Prog. Anal. At. Spectrosc.*, 1982, **5**, 205.
35. Kawaguchi, H., Oshio, Y., and Mizuike, A., *Spectrochim. Acta, Part B*, 1982, **37**, 809.
36. McLaren, J. W., and Mermet, J. M., *Spectrochim. Acta, Part B*, 1984, **39**, 1307.
37. Cresser, M. S., Keliher, P. N., and Wohlers, C. C., *Anal. Chem.*, 1973, **45**, 111.
38. Keliher, P. N., and Wohlers, C. C., *Appl. Spectrosc.*, 1975, **29**, 198.
39. Freeman, G. H. C., Outred, M., and Morris, L. R., *Spectrochim. Acta, Part B*, 1980, **35**, 687.
40. Anderson, D. L., Forster, A. R., and Parsons, M. L., *Anal. Chem.*, 1981, **53**, 770.
41. Forster, A. R., Anderson, D. L., Lovett, R. L., and Parsons, M. L., *Spectrochim. Acta, Part B*, 1981, **36**, 1023.
42. Farnsworth, P. B., and Walters, J. P., *Anal. Chem.*, 1982, **54**, 885.
43. Forster, A. R., Anderson, T. A., and Parsons, M. L., *Appl. Spectrosc.*, 1982, **36**, 499.
44. Anderson, T. A., Forster, A. R., and Parsons, M. L., *Appl. Spectrosc.*, 1982, **36**, 504.
45. Marshall, J., Littlejohn, D., Ottaway, J. M., Miller-Ihli, N. J., O'Haver, T. C., and Harnly, J. M., *Spectrochim. Acta, Part B*, 1984, **39**, 321.
46. Larkins, P. L., *Spectrochim. Acta, Part B*, 1985, **40**, 1585.
47. Hasegawa, T., and Haraguchi, H., *Spectrochim. Acta, Part B*, 1985, **40**, 123.
48. Faires, L. M., and Palmer, B. A., *Spectrochim. Acta, Part B*, 1985, **40**, 135.
49. Sturgeon, R. E., and Chakrabarti, C. L., *Prog. Anal. At. Spectrosc.*, 1978, **1**, 5.
50. Fazakas, J., *Spectrochim. Acta, Part B*, 1982, **37**, 921.
51. Fazakas, J., *Spectrochim. Acta, Part B*, 1983, **38**, 455.
52. Fazakas, J., and Zugravescu, P. G., *Spectrochim. Acta, Part B*, 1988, **43**, 897.
53. Fazakas, J., and Hoenig, M., *Talanta*, 1988, **35**, 403.
54. Fazakas, J., and Zugravescu, P. Gh., *Appl. Spectrosc.*, 1988, **42**, 521.
55. Donega, H. M., and Burgess, T. E., *Anal. Chem.*, 1970, **42**, 1521.
56. Hassell, D. C., Rettberg, T. M., Fort, F. A., and Holcombe, J. A., *Anal. Chem.*, 1988, **60**, 2680.
57. Lovett, R. J., and Parsons, M. L., *Appl. Spectrosc.*, 1977, **31**, 424.
58. O'Haver, T. C., and Kindervater, J. M., *Appl. Spectrosc.*, 1988, **42**, 183.
59. Alkemade, C. Th. J., Hollander, Tj., Snelleman, W., and Zeegers, P. J. Th., "Metal Vapors in Flames," Pergamon Press, Oxford, 1982.

Paper 0/01661F
Received April 12th, 1990
Accepted July 17th, 1990